AMERICAN SOCIETY FOR MICROBIOLOGY | Journal of Virology®

VACCINES AND ANTIVIRAL AGENTS

Rapid Generation of Attenuated Infectious Bursal Disease Virus from Dual-Promoter Plasmids by Reduction of Viral Ribonucleoprotein Activity

Hui Yang,[a] Yu Wang,[a] Chengjin Ye[a]

[a]Department of Veterinary Medicine, College of Animal Science and Technology, Zhejiang A&F University, Hangzhou, Zhejiang Province, China

Hui Yang and Yu Wang contributed equally to this work. Author order was determined alphabetically.

ABSTRACT Infectious bursal disease virus (IBDV) of the *Birnaviridae* family leads to immunosuppression of young chickens by destroying B cells in the bursa of Fabricius (BFs). Given the increasing number of variant IBDV strains, we urgently require a method to produce attenuated virus for vaccine development. To accomplish this goal, the dual-promoter plasmids in which the RNA polymerase II and RNA polymerase I (Pol I) promoters were placed upstream of the IBDV genomic sequence, which was followed by mouse Pol I terminator and a synthetic polyadenylation signal, were developed for rapid generation of IBDV. This approach did not require *trans*-supplementation of plasmids for the expression of VP1 and VP3, the main components of IBDV ribonucleoprotein (RNP). Based on the finding in this study that the IBDV RNP activity was partially retained by VP1-FLAG, we successfully rescued the replication-competent IBDV/1FLAG expressing VP1-FLAG. Compared with its parental counterpart, IBDV/1FLAG formed smaller size plaques in cultured cells and induced the same 100% immune protection *in vivo*. However, neither retarded development nor severe BFs lesion was observed in the IBDV/1FLAG-inoculated chickens. Collectively, this is the first report that viral RNP activity was affected by the addition of an epitope tag on the componential viral proteins. Furthermore, this work demonstrates the rapid generation of attenuated IBDV from dual-promoter plasmids via reducing viral RNP activity by a fused FLAG tag on the C terminus of VP1. This would be a convenient strategy to attenuate epidemic variant IBDV strains for rapid and efficient vaccine development.

IMPORTANCE Immunosuppression in chickens as a result of infectious bursal disease virus (IBDV) infection leads to significant economic losses in the poultry industry worldwide every year. Currently, vaccination is still the best way to prevent the prevalence of IBDV. However, with the occurrence of increasing numbers of variant IBDV strains, it is challenging to develop antigen-matched live attenuated vaccine. Here, we first developed a dual-promoter reverse-genetic system for the rapid generation of IBDV. Using this system, the attenuated IBDV/1FLAG expressing VP1-FLAG, which displays the decreased viral RNP activity, was rescued. Moreover, IBDV/1FLAG inoculation induced a similar level of neutralizing antibodies to that of its parental counterpart, protecting chickens against lethal challenge. Our study, for the first time, describes a dual-promoter reverse-genetic approach for the rapid generation of attenuated IBDV while maintaining entire parental antigenicity, suggesting a potential new method to attenuate epidemic variant IBDV strains for vaccine development.

KEYWORDS IBDV, reverse genetics, RNP, attenuation, vaccine, FLAG tag, VP1, VP3

Infectious bursal disease (IBD) is an acute and contagious disease of young chickens and gives rise to huge amounts of economic losses in the poultry industry worldwide every year. IBD leads to severe immunosuppression by depletion of immature B cells in

Citation Yang H, Wang Y, Ye C. 2020. Rapid generation of attenuated infectious bursal disease virus from dual-promoter plasmids by reduction of viral ribonucleoprotein activity. J Virol 94:e01569-19. https://doi.org/10.1128/JVI.01569-19.

Editor Mark T. Heise, University of North Carolina at Chapel Hill

Copyright © 2020 American Society for Microbiology. All Rights Reserved.

Address correspondence to Chengjin Ye, cjye@zafu.edu.cn.

Received 13 October 2019
Accepted 29 December 2019
Accepted manuscript posted online 8 January 2020
Published 17 March 2020

the bursa of Fabricius (BFs), which is one of the most important central immune organs in young chickens (1). Both broiler and layer flocks are vulnerable to the IBD-induced immunosuppression, resulting in the reduced ability to respond to vaccination, increased susceptibility to the infection with other pathogens, and retarded growth (2).

Infectious bursal disease virus (IBDV) is the causative agent of IBD. IBDV is a nonenveloped virus belonging to the *Birnaviridae* family (3). The viral genome consists of two segments of double-stranded RNA (dsRNA), namely, segment A and segment B. There is one open reading frame (ORF) in segment B, which is about 2.8-kb nucleotides in length, encoding the RNA-dependent RNA polymerase (RdRp) VP1 (4). VP1 is present in virions both as a free polypeptide (VP1) and as a genome-linked protein (VPg) that is covalently linked to the 5′ ends of the genomic RNA segments (5–7), and it is also thought to be involved in the IBDV pathogenicity (8–11). There are two partially overlapping ORFs in segment A, which is about 3.2 kb in length. The smaller ORF encodes the nonstructural protein VP5 which is dispensable for viral replication but engages in virus egress and dissemination (12–17), and the larger ORF encodes a precursor polyprotein, pVP2-VP4-VP3. pVP2-VP4-VP3 is further self-cleaved by VP4 (a serine protease) to yield mature VP2, several small peptides, VP3, and VP4 (18–20). VP2 and VP3 represent the major structural and antigenic components of the capsid. VP2, which harbors the protective antigen containing the neutralizing conformational epitopes, is the major viral structural protein and assembles into 260 trimers to form a $T = 13$ icosahedral IBDV outer capsid (21–23). VP3 constitutes the inner capsid and interacts with both VP1 and viral genomic dsRNA to form a ribonucleoprotein (RNP) complex for facilitating viral encapsulation (24, 25). The RNP complex is also involved in intracellular viral replication and translation (26), during which VP3 significantly stimulates the VP1 RdRp activity (27). Moreover, VP1 and VP3 have been identified to be the minimal set of *trans*-acting factors needed to render the infectivity to IBDV genomic dsRNA (28). In addition, both VP3 and VP4 are considered to be antagonists of interferon-β induction (28–31), and VP3 has also been suggested to act as an antiapoptotic protein that prevents the activation of the cellular dsRNA-dependent protein kinase R (32, 33).

There are two distinct serotypes of IBDV that have been identified, namely, serotype I and II. The serotype I virus is virulent to chickens; however, serotype II virus, which was isolated from turkeys, is nonpathogenic to chickens (34). IBDV is prone to mutate the viral genome during replication, as the fidelity of the RNA viral polymerase is low. Since the identification of the classic strain at the initial area of Gumboro in southern Delaware in 1957 (35), an antigenic variant (36) and a very virulent IBDV strain (37) have emerged. To date, the variant IBDV strain has been identified all over the world (38). Concerningly, the antigenic variant strains can escape the cross-neutralization antisera against the classical strains and the very virulent strains can break through the high level of maternal antibody (39, 40). Vaccination is still currently the best method to prevent IBDV infection. A live attenuated vaccine, which induces the humoral antibody response, cell-mediated cytotoxicity, as well as a mucosal immunoglobulin A response, is superior to a traditional inactivated vaccine (41). With the increasing occurrence of variant IBDV strains (42), it is becoming challenging to develop antigen-matched live attenuated vaccines, and the conventional method to identify the natural attenuated strains cannot meet the urgent requirement.

The reverse genetic system (RGS), a state-of-the-art tool for the generation of recombinant virus, has been increasingly used for vaccine development. For IBDV vaccine development, some investigators have previously rescued recombinant chimeric IBDV by substituting the neutralizing epitopes in the hypervariant region of VP2 in the vaccine strain backbone with those of the variant strains (40, 43). Other groups have inserted the VP2 sequence into an attenuated viral vector to generate a recombinant vaccine (44, 45). Obviously, the disadvantage of these strategies is that some epitopes are missed. Furthermore, the hepatitis delta virus ribozyme sequence, which is used to generate the exact termini in currently available IBDV RGS (46–49), is not as efficient as the RNA polymerase I (Pol I) terminator (50). The rapid RGS is urgently required for IBDV.

In this study, we developed the dual-promoter RGS by combining RNA polymerase II (Pol II) and Pol I upstream of IBDV genomic RNA and placing the mouse Pol I terminator and polyadenylation signal downstream immediately. Combining this with the discovery that a fused FLAG epitope tag on the C terminus of VP1 reduces IBDV RNP activity, we rescued the recombinant IBDV/1FLAG that contains intact segment A and modified segment B, in which FLAG was fused on the C terminus of VP1. Both *in vitro* and *in vivo* experiments confirmed that IBDV/1FLAG is attenuated but maintains all the parental antigenicity required to provide full immune protection, suggesting the possibility of rapid development of antigen-matched live attenuated vaccines from epidemic variant IBDV strains.

RESULTS

Development of dual-promoter plasmids for the generation of IBDV. In our previous study, we found that VP1 and VP3 are required and sufficient for the translation initiation of IBDV genomic RNA and the recovery of infectious virus and that four plasmids are needed for the rescue of IBDV, two of which are for the generation of viral genomic RNA transcripts, and two are for the expression of the minimal set of *trans*-acting factors of VP1 and VP3 (28). To reduce the usage of plasmids and improve the rescue efficiency, we cloned the IBDV plus-sense RNA-generation cassette, which was driven by human Pol I (28), into the region between cytomegalovirus immediate early promoter (CMV) which shows ubiquitous activity in most eukaryotic cells to generate the capped mRNA (51) and polyadenylation signal that stabilizes mRNA (52). As shown in Fig. 1A, the newly generated dual-promoter plasmids were named as p2-mA and p2-mB. Subsequently, Western blot was used to assess the translation of p2-mA and p2-mB in transfected 293T cells, as shown in Fig. 1B. VP3 and VP1 were readily detected in the lysates of 293T cells which were transfected with p2-mA or p2-mB (Fig. 1B, lanes 2 and 4); in contrast, neither VP3 nor VP1 was detected in the lysates of 293T cells that were transfected with p1-mA or p1-mB (Fig. 1B, lanes 1 and 3).

Next, IBDV rescue experiments were performed by cotransfecting 293T cells with the two plasmids (p2-mA and p2-mB) or four plasmids (p1-mA, p1-mB, pVP1, and pVP3). Seventy-two hours posttransfection, the IBDV titer in the supernatant was determined by plaque assay. As shown in Fig. 1C, the mean virus titer in the supernatant of the cells cotransfected with two plasmids is remarkably higher than that of cells cotransfected with four plasmids ($10^{4.5}$ PFU/ml versus $10^{2.0}$ PFU/ml), suggesting higher rescue efficiency with the dual-promoter plasmids. Moreover, the comparison of intracellular replication between the parental virus (IBDV/wild type [WT]) and rescued one (IBDV/rescued) was also carried out by titration of the supernatant over a time course of 96 h with the initial inoculation multiplicity of infection (MOI) of 0.1. As shown in Fig. 1D, the replication kinetics curves of IBDV/WT (circles) and IBDV/rescued (squares) were almost overlapped, indicating that the replication of IBDV/rescued is comparable with its parent IBDV/WT. To further validate the rescued IBDV, the total RNAs from DF-1 cells that were infected with either IBDV/WT or IBDV/rescued were extracted, and reverse transcription-PCR (RT-PCR) was performed to amplify the viral sequence of *vp1* and *vp3*. The purified *vp1* was further conducted to the restriction digestion of PstI, which was introduced into the p2-mB plasmid as a molecular marker by site-directed mutagenesis in advance. The *vp1* amplified from the DF-1 cells, which were infected with IBDV/rescued but not IBDV/WT, was cut into two fragments with the anticipated length (Fig. 1E, lane 3 versus lane 2 in the top panel), and *vp3* was amplified from both infected cells, as expected (Fig. 1E, lanes 2 and 3 in the middle panel).

Together, these data indicate that we have developed a dual-promoter plasmids system for the generation of IBDV without *trans*-supplementation of plasmids for the expression of VP1 and VP3 since the dual-promoter plasmids are also directly translated by the host translational machinery. In addition, the dual-promoter plasmids appear to be more efficient than the four-plasmid system for IBDV rescue.

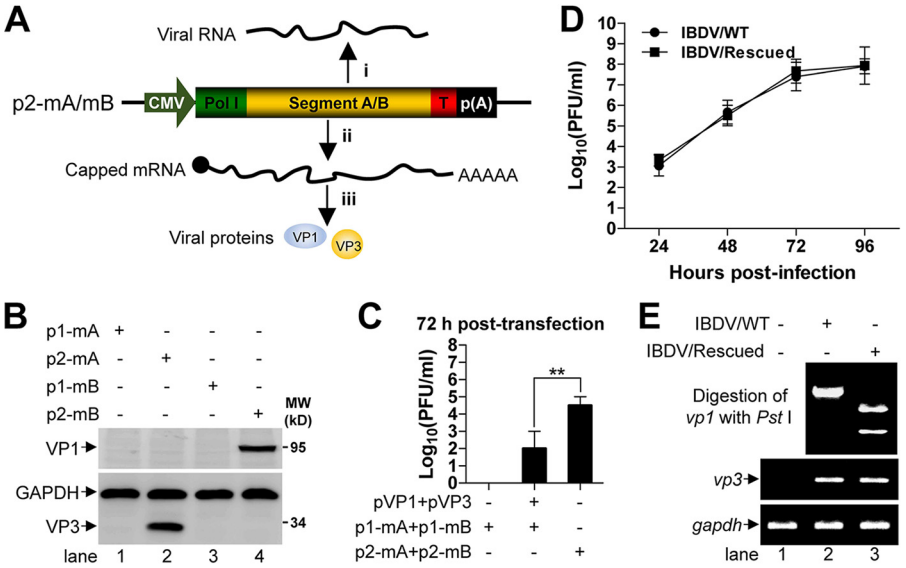

FIG 1 Development of dual-promoter plasmids for the generation of IBDV. (A) Schematic illustration of the intracellular transcription and translation process of the dual-promoter plasmids of p2-mA and p2-mB. After transfection, human Pol I drives the transcription of downstream viral plus-sense RNA, mouse Pol I terminator (T) is used to generate the authentic termini (step i), and CMV drives the transcription of downstream sequences to generate the capped viral mRNA, followed by polyadenosine tail (step ii) for viral protein translation using the cellular translational machinery (steps iii). (B) Monolayer of 293T cells (6-well format) were transfected with the indicated plasmids (4 μg each) for 72 h, then the whole-cell lysate was analyzed by Western blot using the antibodies against VP1 and VP3, and GAPDH was probed as a loading control. (C) The IBDV titers in the supernatant of 293T cells (triplicates in 6-well plate) transfected with the indicated plasmids (1 μg of each plasmid, the total mass of plasmids for each group was made to be 4 μg by adding pCI-neo vector DNA) were determined by plaque assay at 72 h posttransfection. Data were presented as mean $\pm$ SD. **, $P < 0.01$. (D) Monolayer of DF-1 cells (triplicates in 6-well plate) were infected with IBDV/WT or IBDV/rescued at an MOI of 0.1, and the virus titers in the supernatant were determined by plaque assay at the indicated times. Data were presented as mean $\pm$ SD. (E) Monolayer of DF-1 cells (6-well format) were infected with IBDV/WT or IBDV/rescued at an MOI of 1 for 12 h, and then the total RNA was extracted for RT-PCR analysis of *vp1*, *vp3*, and *gapdh*. The gel-purified fragments of *vp1* (1 μg) were further conducted to PstI digestion. All the DNA fragments were separated on a 1% agarose gel.

FLAG tag fused on the C terminus of VP1 reduces IBDV RNP activity. FLAG tag, which is composed of 8 amino acids (DYKDDDDK), is a commonly used artificial epitope in molecular biology research. The detection of FLAG is used to represent the target protein when there is no commercial antibody available and is made possible by fusion expression of the FLAG tag on the C or N terminus. Here, we investigated whether the FLAG tag affects the RNP activity which is indispensable for IBDV genomic RNA translation initiation by using the different combinations of various VP1 and VP3 which were tagged with FLAG on the C or N terminus (Fig. 2A). The plasmid of p1-RmA (28), which generates the minus-sense IBDV segment A transcript after transfection into 293T cells, was employed to evaluate the IBDV RNP activity by checking the expression of VP4 (19). As shown in Fig. 2B, VP4 was detected in the lysate of 293T cells that were cotransfected with the plasmids of pVP1-FLAG, pVP3, and p1-RmA or pVP1, pFLAG-VP3, and p1-RmA and positive control (cotransfection of pVP1, pVP3, and p1-RmA) (Fig. 2B, lanes 5, 2, and 1) but not in the lysate of cells cotransfected with other plasmid combinations (pVP1/pVP3-FLAG/p1-RmA or pFLAG-VP1/pVP3/p1-RmA) (Fig. 2B, lanes 3 and 4). Moreover, the expression level of VP4, which represents the activity of IBDV RNP, was reduced by about 70% in the 293T cells that were cotransfected with the plasmid of pVP1-FLAG, pVP3 and p1-RmA compared with that of the positive control (Fig. 2C, bar 5 versus bar 1). Reciprocally, we also tested whether VP1/VP3 could mediate the translation of the plus-sense transcript of mBFLAG, in which the FLAG tag coding sequence was fused immediately downstream of the VP1 ORF (Fig. 2D). A single band with the anticipated molecular weight in the Western blot membrane was detected in

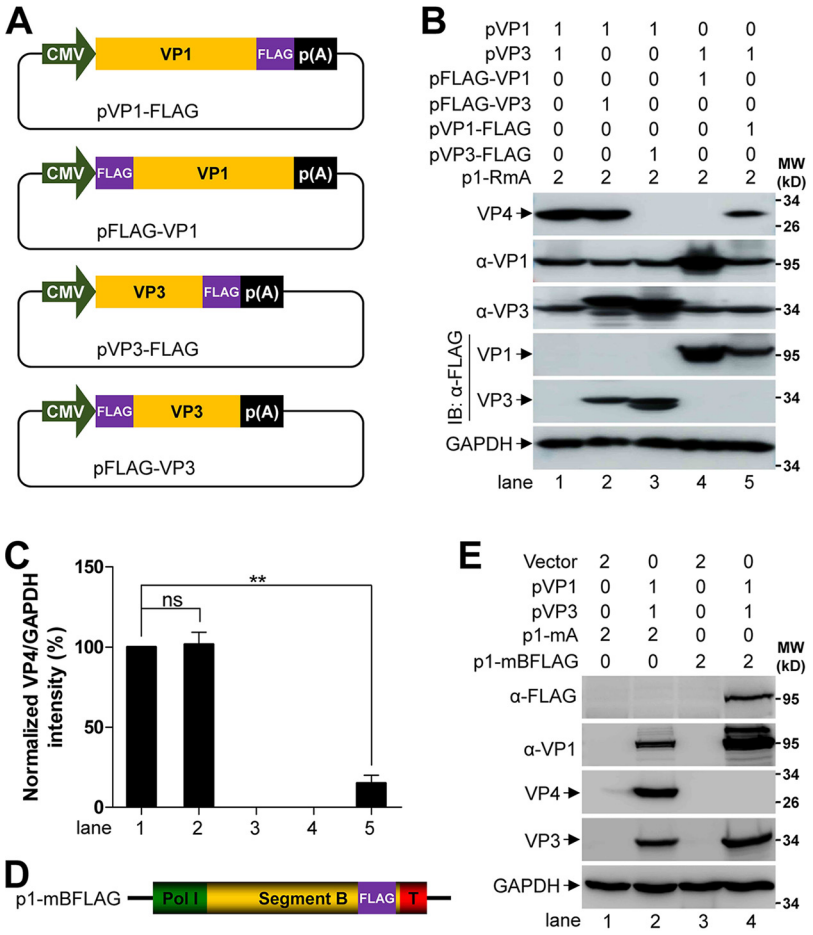

FIG 2 FLAG tag fused on the C terminus of VP1 reduces IBDV RNP activity. (A) Schematic representation of the plasmids of pVP1-FLAG, pFLAG-VP1, pVP3-FLAG, and pFLAG-VP3. CMV and p(A) stands for cytomegalovirus immediate early promoter and polyadenylation signal, respectively. (B) Monolayer of 293T cells (6-well format) were cotransfected with the indicated plasmids, and the amount of each plasmid is indicated above the lanes (in microgram). Then, the whole-cell lysate was analyzed by Western blot using the antibodies against VP1, VP4, VP3, and FLAG at 72 h posttransfection, and GAPDH was probed as a loading control. (C) Comparison of the expression level of VP4 in different lanes in panel B. The optical density of VP4 and GAPDH was quantified by Quantity One software, and the value of VP4 over GAPDH in the lane 1 of panel B was normalized as 100%. Data were presented as mean ± SD. ns, not significant; **, $P < 0.01$. (D) Schematic representation of the constitution of p1-mBFLAG. Pol I and T stands for human RNA polymerase I promoter and mouse Pol I terminator, respectively. FLAG tag was fused on the C terminus of VP1. (E) Monolayer of 293T cells (6-well format) were cotransfected with the indicated plasmids, and the amount of each plasmid is indicated above the lanes (in microgram). Then, the whole-cell lysate was analyzed by Western blot using the antibodies against VP1, VP4, VP3, and FLAG at 72 h posttransfection, and GAPDH was probed as a loading control.

the lysate of 293T cells that were cotransfected with pVP1, pVP3, and p1-mBFLAG by incubating with the FLAG monoclonal antibody (MAb) (Fig. 2E, lane 4 in the top panel), which was also recognized by the VP1 antibody (Ab) (Fig. 2E, lane 4 in the second top panel).

These results demonstrate that the N-terminal FLAG-tagged VP1 (FLAG-VP1) and the C-terminal FLAG-tagged VP3 (VP3-FLAG) abolish the activity of IBDV RNP; however, the N-terminal FLAG-tagged VP3 (FLAG-VP3) maintains the complete IBDV RNP activity and the C-terminal FLAG-tagged VP1 (VP1-FLAG) significantly reduces the IBDV RNP activity. Moreover, the FLAG tag fused on the C terminus of VP1 is also accepted to be translated from the recombinant viral genome of mBFLAG by IBDV RNP.

Generation of recombinant IBDV-expressing VP1-FLAG. Given that the FLAG tag could acceptably be fusion expressed on the C terminus of VP1 by IBDV RNP while retaining partial IBDV RNP activity, we sought to rescue recombinant IBDV expressing

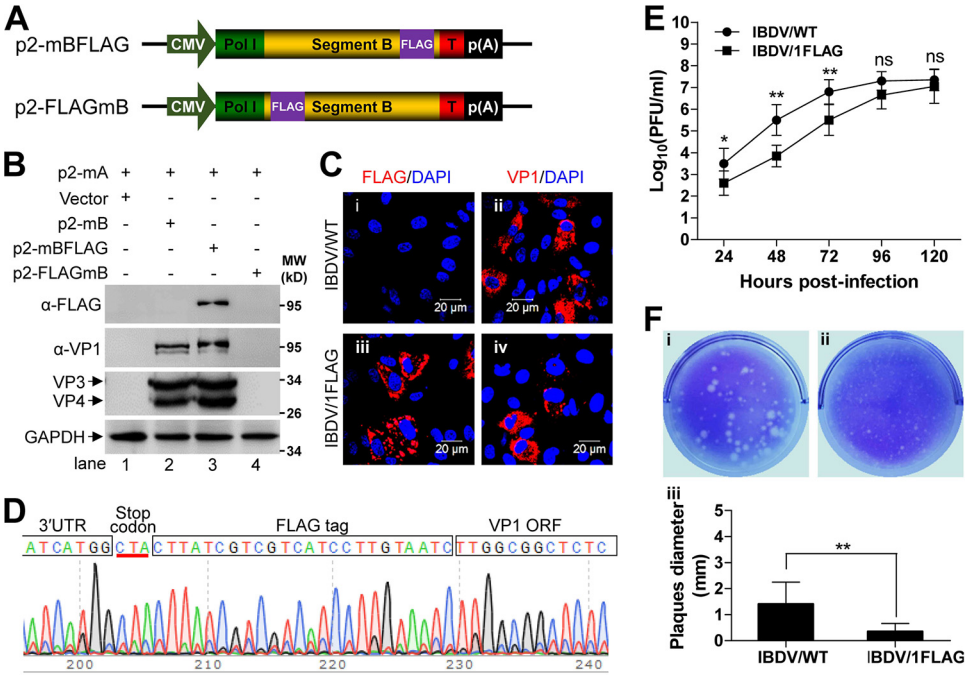

FIG 3 Generation of recombinant IBDV expressing VP1-FLAG. (A) Schematic representation of the plasmids of p2-mBFLAG and p2-FLAGmB. CMV and Pol I stands for cytomegalovirus immediate early promoter and human Pol I promoter, respectively. T represents mouse Pol I terminator and p(A) stands for polyadenylation signal. (B) The supernatant of the 293T cells (6-well format) which were cotransfected with the indicated plasmids (2 μg of each plasmid in each group) for 72 h was passaged 3 times in DF-1 cells. Finally, the DF-1 whole-cell lysate was analyzed by Western blot using the antibodies against FLAG, VP1, and VP3, and GAPDH was probed as a loading control. (C) After implantation of DF-1 cells on the coverslip in 6-well plate, cells were infected (MOI, 1) with IBDV/WT or IBDV/1FLAG for 12 h, and then fixed and immunostained with the antibodies against VP1 (left column) or FLAG (right column), followed by the staining with Alexa Fluor-568-labeled secondary antibody. Nucleus was stained with DAPI. Scale bars = 20 μm. (D) After passage of IBDV/1FLAG in DF-1 cells for 30 times, the full length of viral segment B was amplified by RT-PCR and further used for Sanger sequencing. The chromatogram was screenshot to show the existence of FLAG tag sequence (full box) between VP1 ORF and 3′ untranslated region (UTR) (opened boxes), and the stop codon was underlined in red. (E) Monolayer of DF-1 cells (triplicates in 6-well plate) were infected with IBDV/WT or IBDV/1FLAG at an MOI of 0.1; the virus titers in the supernatant were determined by plaque assay at the indicated times. Data were presented as mean ± SD. ns, not significant; *, $P < 0.05$; **, $P < 0.01$. (F) The representative plaques formed by IBDV/WT (i) or IBDV/1FLAG (ii) in the monolayer of DF-1 cells (6-well format) were stained with 1% crystal violet at 96 h postinfection, and the histogram (iii) was plotted based on the diameter of 30 arbitrary plaques formed by IBDV/WT or IBDV/1FLAG. Data were presented as mean ± SD. **, $P < 0.01$.

VP1-FLAG. To avoid the possible recombination with the *trans*-supplemented expression plasmid of pVP1, we employed the dual-promoter IBDV rescue system to construct the dual-promoter plasmids of p2-mBFLAG, in which FLAG tag was fused on the C terminus of VP1 and p2-FLAGmB in which FLAG was fused on the N terminus of VP1 as a control (Fig. 3A). Then, the virus rescue experiment was performed in 293T cells by cotransfection of p2-mA accompanied with either p2-mBFLAG or p2-FLAGmB. Cotransfection of p2-mA and p2-mB was included as a positive control. As shown in Fig. 3B, a specific band reacting with FLAG MAb was detected in the lysate of DF-1 cells that were inoculated with the supernatant of the 293T cells cotransfected with p2-mA and p2-mBFLAG (Fig. 3B, lane 3 in top panel). Of note, the VP1-FLAG was also recognized by incubating with the VP1 Ab. Because of the fusion expression, the blot band of VP1-FLAG was slightly higher than that of VP1 (Fig. 3B, lane 3 versus lane 2 in the second top panel). In addition, we employed a immunofluorescent assay to assess the expression of VP1 and VP1-FLAG in DF-1 cells infected with either IBDV/WT or IBDV/1FLAG. Fluorescent signal mediated by VP1 Ab was detected in both DF-1 cells that were infected with IBDV/WT or IBDV/1FLAG (Fig. 3C, frames ii and iv), while the signal mediated by FLAG MAb was detected in the IBDV/1FLAG-infected DF-1 cells but not in

the IBDV/WT-infected DF-1 cells (Fig. 3C, frame iii versus frame i). These data indicate that the recombinant virus of IBDV/1FLAG is replication competent.

To verify the stability of the FLAG tag in the IBDV/1FLAG genome, the full length of IBDV/1FLAG segment B was amplified from virus fluid that had been passaged 30 times in DF-1 cells and used for Sanger sequencing. The sequencing data revealed that the FLAG tag sequence still existed in the frame of VP1 ORF immediately upstream of the stop codon (Fig. 3D, full box). To characterize the recombinant IBDV/1FLAG, we compared its intracellular replication with that of its parental counterpart. As shown in Fig. 3E, in the beginning period (before 72 h), the growth of IBDV/1FLAG was slower than that of IBDV/WT ($10^{5.5}$ PFU/ml versus $10^{6.8}$ PFU/ml at 72 h postinfection); however, the average virus titer was getting closer to that of IBDV/WT at the later period ($10^{7.1}$ PFU/ml versus $10^{7.4}$ PFU/ml at 120 h postinfection). Importantly, the size of the plaques formed by IBDV/IFLAG in DF-1 cells (Fig. 3F, frame ii) was significantly smaller than those formed by IBDV/WT (Fig. 3F, frame i), as measured by mean diameter (0.35 mm versus 1.42 mm) (Fig. 3F, panel iii) at 96 h postinfection.

Collectively, these results reveal that the recombinant IBDV/1FLAG expressing VP1-FLAG was successfully rescued based on the dual-promoter plasmids system, which formed significantly smaller plaques than that of IBDV/WT in cultured DF-1 cells, implying the attenuated pathogenicity of IBDV/1FLAG.

Attenuation of IBDV pathogenicity by fusing FLAG tag on the C terminus of VP1. Because the size of the plaques formed in cultured DF-1 cells by IBDV/1FLAG was remarkably smaller than that formed by IBDV/WT, it is most probable that the recombinant virus was attenuated. To test this hypothesis, we compared the pathogenicity of IBDV/1FLAG between IBDV/WT by inoculation of 1-week-old specific-pathogen-free (SPF) chickens. The chickens were inoculated with 10^4 PFU each (IBDV/WT or IBDV/1FLAG) or Dulbecco modified Eagle medium (DMEM) (0.2 ml each) through ocular drop administration. At 14 days postinoculation, the BFs were isolated from sacrificed chickens after determination of body weight. In contrast with the DMEM control treatment, IBDV/WT inoculation hampered chicken development that was reflected by the significantly decreased mean of chicken body weight (222.7 g versus 165.6 g, respectively); however, the IBDV/1FLAG inoculation had no significant effect on the mean of chicken body weight (220.6 g versus 222.7 g, respectively) (Fig. 4A, panel i). Moreover, the mean of the bursa weight divided by the bodyweight (B/B ratios) of chickens inoculated with IBDV/WT was significantly decreased compared with chickens inoculated with DMEM or IBDV/1FLAG (0.0022 versus 0.0050 or 0.0048, respectively) (Fig. 4A, panel ii). Furthermore, the mean of (B/B ratio of challenged chicken)/(mean B/B ratio of uninfected control group) (B/B index) of chickens inoculated with DMEM, IBDV/WT, or IBDV/1FLAG was also calculated with the results of 1.00, 0.43, and 0.97, respectively, and the BFs was considered atrophied when this value was less than 0.70 (53) (Fig. 4A, panel iii). Consistent with the B/B index, inoculation of IBDV/WT led to significantly atrophied BFs (Fig. 4B, middle row versus top row); however, IBDV/1FLAG inoculation had no significant effect on the size of BFs (Fig. 4B, bottom row versus top row). In addition, the interior wrinkle was clear and the surface was clean with light color in the representative BF from chicken inoculated with DMEM or IBDV/1FLAG (Fig. 4C, frames i and iii), except for slight hemorrhagic points appearing on the surface of BFs of chicken inoculated with IBDV/1FLAG (Fig. 4C, circled in frame iii). In contrast, the BFs of chickens inoculated with IBDV/WT appeared darker in color, which was hemorrhage, the wrinkle in the interior of BF became indistinct, and many hemorrhagic sites were still on the surface (Fig. 4C, squared in frame ii).

To verify the expression of VP1-FLAG and VP1 in the BFs, histological sections of BFs of the chickens inoculated with DMEM, IBDV/WT, or IBDV/1FLAG were studied by immunofluorescent staining using VP1 and FLAG antibodies. As shown in Fig. 4D, fluorescent signal from both VP1 and FLAG was detected in the BFs sections of chickens inoculated with IBDV/1FLAG (Fig. 4D, frames i and k in panel i); however, only VP1 was only detected in the BFs of chickens inoculated with IBDV/WT (Fig. 4D, frame g in panel i). Additionally, the deletion of cells in IBDV/1FLAG-infected BFs, which was reflected by

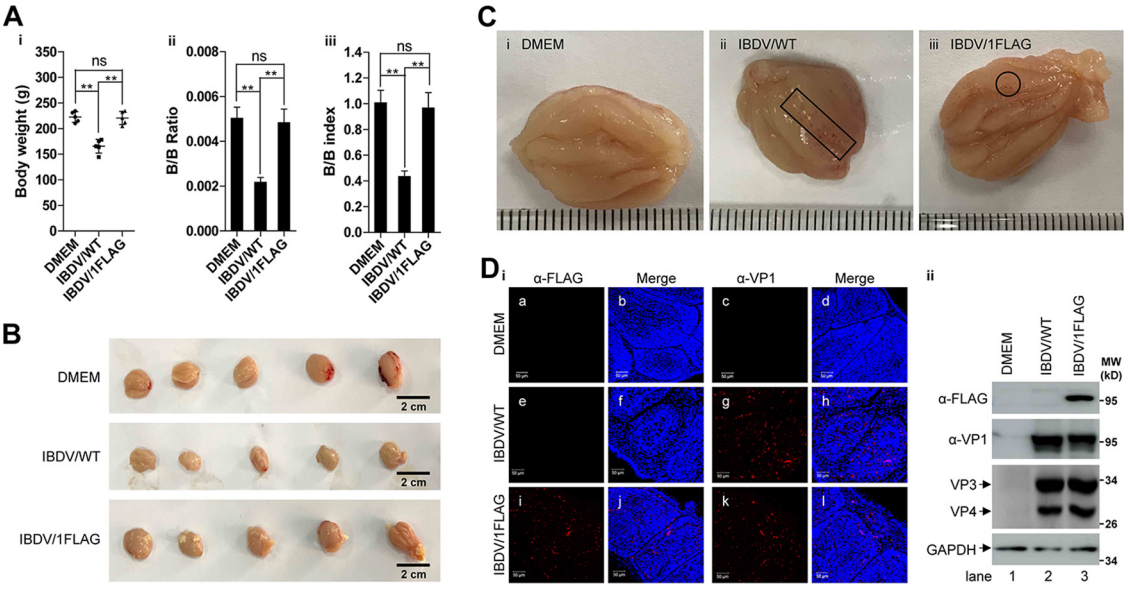

FIG 4 Attenuation of IBDV pathogenicity by fusing FLAG tag on the C terminus of VP1. (A–C). One-week-old SPF chickens (5 in each group) were inoculated with DMEM (0.2 ml each), IBDV/WT (10^4 PFU each), or IBDV/1FLAG (10^4 PFU each) through eye dropping. After 14 days of regular isolated feeding, the bodyweight was determined before sacrifice (Ai), the BFs was isolated and weighed and the weight ratio of BFs to bodyweight (B/B ratio) was calculated (Aii), and the B/B index was determined (Aiii) according to the method described in the section of Materials and Methods; at the same time, the images of the overall BFs appearance (B) and the interior of representative BFs of chickens inoculated with DMEM (Ci), IBDV/WT (Cii), or IBDV/1FLAG (Ciii) were photographed, and the hemorrhagic sites or the single hemorrhagic points were squared or circled in the BFs interior representative images. Scale bar in panel B stands for 2 cm, and the distance between two adjacent lines in panel C is 1 mm. Data were presented as mean ± SD. ns, not significant; **, $P < 0.01$. (D) The BFs sections of chickens inoculated with DMEM, IBDV/WT, or IBDV/1FLAG were immunostained with the antibodies against FLAG (frames a, e, and i) or VP1 (frames c, g, and k) followed by staining with Alexa Fluor-568-labeled secondary antibody, and the nucleus was stained with DAPI (panel i). Scale bars = 50 μm. The whole lysate of the BFs, which were from the chickens inoculated with DMEM, IBDV/WT, or IBDV/1FLAG, was also subjected to Western blot analysis by using the antibodies against FLAG, VP1, VP3, and VP4, and GAPDH was probed as a loading control (panel ii).

the 4′,6-diamidino-2-phenylindole (DAPI)-positive signal was significantly less than that of IBDV/WT-infected ones (Fig. 4D, frames j and l versus frames f and h). DAPI signal in IBDV/1FLAG-infected BFs was comparable to that of DMEM-inoculated controls (Fig. 4D, frames j and l versus frames b and d, respectively). Consistently, VP1-FLAG was only detected in the whole lysate of BFs of IBDV/1FLAG-inoculated chickens; and VP1, VP3, and VP4 were detected in the lysate of BFs of the chickens inoculated with either IBDV/WT or IBDV/1FLAG (Fig. 4D, panel ii).

These results indicate that IBDV/WT inoculation leads to BFs atrophy in 1-week-old SPF chickens, and IBDV/1FLAG that expresses VP1-FLAG during infection alleviates the viral pathogenicity and chicken retarded development.

Recombinant IBDV/1FLAG maintains the parental antigenicity. Although the attenuation of IBDV/1FLAG in cultured cells and *in vivo* has been observed, it is still uncertain whether IBDV/1FLAG maintains the antigenicity of its parental counterpart. To address this question, we first compared the morphology of IBDV/1FLAG and IBDV/WT, which is the basis of antigenicity. As shown in Fig. 5A, both IBDV/WT and IBDV/1FLAG displayed the typical icosahedral symmetry and similar size (~50 nm in diameter) (Fig. 5A, indicated by arrows in frames i and ii). Next, we conducted an animal experiment to compare the antigenicity of IBDV/1FLAG and IBDV/WT *in vivo* (Fig. 5B). Five 1-week-old SPF chickens in each group were inoculated with IBDV/WT (10^4 PFU each), IBDV/1FLAG (10^4 PFU each), or DMEM (0.2 ml each) through eye dropping, and the antibody in the serum was tested at 0, 7, 14, and 21 days postinoculation (dpi) by enzyme-linked immunosorbent assay (ELISA). As shown in Fig. 5C, IBDV/WT inoculation induced slightly higher mean antibody titers than IBDV/1FLAG, but this difference was not statistically significant (1,000 versus 680 at 7 dpi, 2,320 versus 1,840 at 14 dpi, and 2,560 versus 2,240 at 21 dpi, respectively). At 21 dpi, all the chickens were challenged

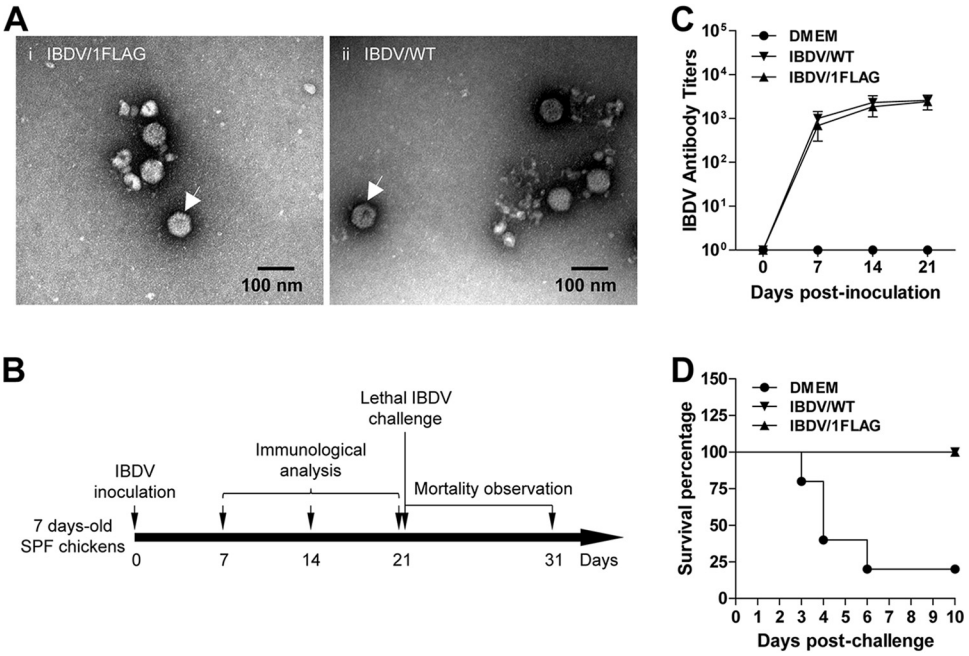

FIG 5 Recombinant IBDV/1FLAG maintains the parental antigenicity. (A) Transmission electron microscopy analysis of the morphology of IBDV/1FLAG (i) and IBDV/WT (ii); scale bars = 100 nm. (B) Schedule for comparison of the viral antigenicity between IBDV/1FLAG and IBDV/WT. (C and D) The neutralizing antibody levels in the serum of chickens (5 in each group) inoculated with DMEM (0.2 ml each), IBDV/WT (10^4 PFU each), or IBDV/1FLAG (10^4 PFU each) were tested at 0, 7, 14, and 21 days postinoculation, and the curve was plotted based on the ELISA results (C). Then, all the chickens were challenged by intranasal dropping of IBDV BC6/85 (2×10^4 EID_{50} each) at 21 days postinoculation of DMEM, IBDV/WT, or IBDV/1FLAG, and the survival curves were generated by daily observing the mortality for 10 days according to the method of Kaplan-Meier (D).

by inoculation of virulent IBDV strain BC6/85 at the dose of 2×10^4 50% egg infective dose (EID_{50}) per individual through intranasal drops. At 10 days postchallenge, both IBDV/WT and IBDV/1FLAG inoculation provided complete immune protection against lethal challenge (Fig. 5D, inverted triangle and regular triangle which are overlapped), in stark contrast to 80% mortality in the DMEM control-treated chickens (Fig. 5D, circles).

These results demonstrate that IBDV/1FLAG, which possesses the same morphology as IBDV/WT, also induces a similar neutralizing antibody as that of its parental counterpart to provide complete immune protection against a subsequent lethal challenge, indicating the adequate parental antigenicity is maintained in IBDV/1FLAG.

DISCUSSION

In this study, we described a dual-promoter reverse genetic system for the rapid generation of IBDV. The dual-promoter system was first used for the rescue of influenza virus (54). Influenza is a negative-sense RNA virus. The IBDV genome is dsRNA and the human Pol I-driven IBDV positive-strand RNA has been applied to the successful rescue of IBDV (28). Therefore, we engineered the Pol II and Pol I in the same strand (Fig. 1A). CMV, which is one kind of Pol II promoter, was placed in front of Pol I to ensure the transcription of downstream sequences to generate capped mRNAs which are translated into viral proteins (Fig. 1B), although some research has shown that this kind of combination of promoters leads to lower virus yield (55). By using this strategy, however, we no longer need to prepare the helper plasmids that are used for the expression of VP1 and VP3. Importantly, the IBDV rescue efficiency using two dual-promoter plasmids was significantly higher than that using four plasmids (Fig. 1C), at least partially due to the higher transfection efficiency. Additionally, because of the species specificity of Pol I promoter (56), the human Pol I needs to be substituted by an avian Pol I promoter if we want to apply the dual-promoter IBDV rescue plasmids in

DF-1 cells. This work opened a new avenue for the development of an optimized rescue system for other dsRNA viruses, such as reovirus.

Epitope tags, such as FLAG, hemagglutinin (HA), MYC, and V5, are popularly used in virus research. These tags are commonly thought to have no effect on the function of target proteins. For instance, the arenaviral RNP activity is not affected by fusion expression of the epitope tags (FLAG or HA) on either N or C terminus of the viral proteins L and NP (57, 58). Although we have shown that FLAG-VP1 still interacts with VP3 (30), FLAG-VP1 and VP3-FLAG are found to result in incompetent IBDV RNP activity in this study (Fig. 2B). However, FLAG-VP3 does not affect IBDV RNP activity, which was decreased by about 70% by VP1-FLAG (Fig. 2C). In light of these findings, we should be cautious of the use of epitope-tagged IBDV viral proteins as a direct representation of original ones, especially for experiments to evaluate IBDV RNP activity. We speculate that FLAG tag affects the structural conformation of VP1 and VP3 and the catalytic activity of the complex has been changed. However, further investigations are still needed to elucidate the mechanism. Besides the smaller size plaques formed by IBDV/1FLAG (Fig. 3F), it also exhibited lower pathogenicity than its parental counterpart *in vivo* (Fig. 4A to C). Regarding attenuation mechanisms, one possibility is that the expression model of VP1 was changed because there were two bands on a VP1 Western blot and only one band was detected by incubation with FLAG MAb (Fig. 3B). Noticeably, the distribution pattern of VP1 and VP1-FLAG seems different too (Fig. 3C, frame ii versus frame iii). The other possibility is that the existence of the FLAG tag increases the burden of segment B expression; assuming that the VP1 amount is the rate-determining step for IBDV assembly, it needs more time to accomplish the replication of VP1-FLAG than VP1, which is also supported by the slower replication of IBDV/1FLAG in the early stage (Fig. 3E). Meanwhile, the lower increase of intracellular c-Src kinase phosphorylation, which is a prerequisite for IBDV cellular entry, may also contribute to this (59) because the viral load in the BFs of the chickens infected with IBDV/1FLAG is less than that of IBDV/WT (Fig. 4D).

Rapid generation of an antigen-matched live attenuated vaccine is currently the best method to reduce the prevalence of variant IBDV strains. Fusion of a FLAG tag on the C terminus of VP1 causes no significant change in the IBDV morphology (Fig. 5A), solidifying the possibility to attenuate epidemic variant IBDV strains by fusing a FLAG tag on the C terminus of VP1. The parental IBDV used in this study shares more than 99.5% identity with the commercial vaccine strain B87, which is a vaccine of medium virulence that is still pathogenic to newborn chickens (60). In this study, we aimed to investigate whether the pathogenicity and antigenicity were changed by fusing FLAG tag on the C terminus of VP1. The IBDV/1FLAG inoculation induced a similar level of neutralizing antibodies, compared with WT virus (Fig. 5B), indicating that the viral antigenicity was not altered. Neither BFs atrophy (Fig. 4B) nor developmental retardation (Fig. 4A) was observed by inoculation of IBDV/1FLAG, suggesting it is attenuated and that VP1 is involved in the IBDV pathogenicity (8, 10, 11). Another potential advantage of the attenuated IBDV/1FLAG is to distinguish the chickens of the attenuated vaccine immunization and the wild-type virus infection by checking for the anti-FLAG antibody in the serum, as a previous report showed the induction of HA antibody in chickens inoculated with the IBDV expressing VP1-HA (61).

In conclusion, we developed a dual-promoter plasmid system, in which the Pol II and Pol I promoters were organized in the same direction, for rapid IBDV rescue without providing extra plasmids for the expression of VP1 and VP3. Using this system, we rescued IBDV/1FLAG expressing VP1-FLAG, which leads to lower IBDV RNP activity. Despite the attenuated pathogenicity, IBDV/1FLAG reserves all the antigenicity of its parental counterpart, suggesting that this may be a promising method to generate attenuated epidemic variant IBDV strains for live vaccine development.

MATERIALS AND METHODS

Cell lines, virus, and reagents. HEK293T cells (ATCC CRL-11268) and the chicken fibroblast cell line DF-1 (ATCC CRL-12203) were routinely maintained as previously described (28). A DF-1 cell-adapted IBDV

strain (IBDV/WT) (GenBank accession numbers MF083701.1 and MF083702.1) which shares more than 99.5% identity in both levels of amino acids and nucleotides with the IBDV vaccine strain B87 was used in this study. The standard virulent IBDV BC6/85 strain was used for challenge studies, which was purchased from the China Institute of Veterinary Drug Control. Mouse anti-VP1, mouse anti-VP3, and mouse anti-VP4 polyclonal antibodies were generated from the serum of mice by immunizing them with prokaryotic-purified VP1, VP3, and VP4, respectively. Mouse anti-GAPDH MAb was purchased from BioBEST Biotechnology (Anhui, China). The IBDV Ab ELISA kit, in which the whole inactivated virus particles were coated as antigen, was supplied by IDEXX (Westbrook, ME, USA).

RT-PCR and PstI digestion. The total RNA was extracted by TRIzol (Thermo Fisher, Waltham, MA, USA) according to the manufacturer's instruction for RT-PCR amplifications of *vp1*, *vp3*, and *gapdh* by using PrimeScript II high-fidelity RT-PCR kit (TaKaRa, Dalian, China), and the PstI digestion of *vp1* was performed according to a previous description (28). All the DNA products were subjected to 1% agarose gel electrophoresis analysis and the photograph was taken under the gel documentation and imaging analysis system. Alternatively, the full length of amplified segment B was recovered by the gel purification kit (TaKaRa) and used for Sanger sequencing. All the primer sequences used for RT-PCR are available on request.

Plasmid construction, site-directed mutagenesis, and transfection. The full length genomes of segment A and segment B were amplified from the IBDV/WT genome by RT-PCR, and the plasmids of p1-mA, p1-mB, and p1-RmA were generated as previously described (28). p2-mA/mB were constructed by cloning the cassette used for plus-sense IBDV genomic RNA generation in the p1 plasmid into the region between the CMV promoter and synthetic polyadenylation signal by the restriction sites of NheI and MluI according to the standard protocol of the gene engineering technique. The site-directed mutagenesis kit (Agilent, Santa Clara, CA, USA) was used to introduce the PstI restriction site in p2-mB (1,787 nucleotide [nt] in *vp1*) as a molecular marker. The plasmids of p2-mBFlag and p2-FlagmB were generated based on the backbone of p2-mB by inverse PCR (62). The ORFs of VP1 and VP3 were inserted into pCI-neo (Promega, Fitchburg, WI, USA), pCMV-FLAG-N (Clontech, Mountain View, CA, USA), and pCMV-FLAG-C (Clontech) to generate the expression plasmids of pVP1, pVP1-FLAG, pFLAGA-VP1, pVP3, pVP3-FLAG, and pFLAG-VP3. All plasmids were confirmed by Sanger sequencing, and all the primer sequences used for plasmid construction are available on request. Transfection of plasmids into cells was performed with a transfection reagent (BioBEST) according to the manufacturer's instruction. Briefly, the plasmids (4 μg in total) were diluted by 400 μl of Opti-MEM (Thermo Fisher) in an Eppendorf tube, and after a 5-min incubation at room temperature, 10 μl of the transfection reagent was added and mixed thoroughly with the DNA solution by pipetting up and down. After another 20-min incubation at room temperature, the mixture was dropwise added onto the monolayer of 293T cells (6-well plate format, 10^6 cells/well), and then the cells were further cultured at 37°C in an incubator until the desired time. The amounts of plasmids in the different groups were kept constant by using pCI-neo vector DNA.

Western blot. The extraction of whole-cell lysate, the SDS-PAGE separation, and Western blot were performed as previously described (30). Briefly, the whole-cell lysate was extracted by lysis buffer (50 mM Tris-HCl [pH 7.4], 150 mM NaCl, 1% Triton X-100, and 1% sodium deoxycholate) at 4°C for 30 min, followed by centrifugation at 12,000 $\times$ *g* at 4°C for another 30 min. Equivalent amounts of cell lysate were subjected to 12% SDS-PAGE and transferred to nitrocellulose membranes. After blocking with 5% bovine serum albumin in phosphate-buffered saline (PBS) containing 0.1% Tween 20 (PBST) at room temperature for 1 h, the membranes were incubated with primary antibodies at 4°C overnight and followed by horseradish peroxidase-conjugated secondary antibody incubation at 37°C for 1 h. The blots were developed with the ECL detection reagent (BioBEST) in the MiniChemi 420 system (Sage Tech, Beijing, China), and the GAPDH was probed as the loading control. Finally, the blots were scanned, and densitometric quantification analysis was performed by using Bio-Rad Quantity One software.

Plaque assay. The plaque assay for IBDV/WT and IBDV/1FLAG in DF-1 cells was performed as described previously (59). Briefly, the serial 10-fold dilution samples (0.1 ml aliquots of each dilution) of IBDV/WT or IBDV/1FLAG (passage 30) were inoculated onto the monolayer of DF-1 cells in the 6-well plates. After incubating at 37°C for 1 h for the virus internalization, the cells were covered with 1% low melting agarose after 3-times PBS wash. Finally, the cells were stained with 1% crystal violet at 96 h postinfection, the titer was determined by counting the plaques induced, and the representative images were photographed. The mean of plaque size was determined by measuring the diameter of 30 arbitrary plaques.

Confocal laser scanning microscopy. DF-1 cells in chamber slides were infected with IBDV/WT or IBDV/1FLAG (passage 30) (MOI, 1) for 12 h. Then, the cells were fixed in 4% prechilled paraformaldehyde (PFA) solution overnight at 4°C, permeabilized with 0.1% TritionX-100 in PBS after a 3-times extensive wash, and incubated with mouse anti-VP1 or mouse anti-FLAG at 37°C for 1 h, followed by staining with Alexa Fluor-568-labeled donkey anti-mouse IgG for another 1 h at 37°C, and the nucleus was stained with 4′,6-diamidino-2-phenylindole (DAPI). For the immunostaining of paraffin-embedded sections, the deparaffinized sections were inoculated with anti-VP1 or anti-FLAG at 37°C for 1 h, followed by staining with Alexa Fluor-568-labeled donkey anti-mouse IgG for another 1 h at 37°C, and the nucleus was stained with DAPI. All the images were acquired on a Zeiss LSM 510 inverted confocal microscope using the proper excitation laser wavelength.

Transmission electron microscopy. Both IBDV/WT and IBDV/1FLAG (passage 30) were propagated in DF-1 cells and purified crudely by pelleting through a 25% (wt/wt) sucrose cushion twice at 150,000 $\times$ *g* for 3 h at 4°C. Samples were applied to glow-discharged carbon-coated grids for 2 min and then stained with 2% aqueous uranyl acetate (63). Micrographs were acquired with a TecnaiG2 Spirit 120 kV electron microscope operating at a magnification of $\times$120,000.

Animal experiments. All the fertilized specific-pathogen-free (SPF) chicken eggs were purchased from Hangzhou Jianliang Biotechnology Co., Ltd. and were hatched at 37°C in an incubator. The chickens were maintained in isolators that were supplied with a filtered intake and exhaust air. All animal experiments were carried out under the approval of the Animal Ethics Committee of Zhejiang A&F University (number ZAFU-2017-004).

Pathogenicity test. Five 1-week-old SPF chickens in each group were inoculated with DMEM (0.2 ml each), IBDV/WT (10^4 PFU each), or IBDV/1FLAG (passage 30; 10^4 PFU each) through eye dropping. Fourteen days later, chicken bodyweights were determined before sacrifice; the BFs was isolated, weighed, and photographed; and then the BFs were split into the following two pieces: one was fixed in 4% PFA for preparing the histological sections and another one was used for Western blot analysis. The bursa: bodyweight ratio (B/B ratio) was determined for each chicken by dividing the bursa weight over the bodyweight, and the B/B index was then calculated by the formula (B/B ratio of challenged chicken)/(mean B/B ratio of uninfected control group); bursa were considered atrophied when their B/B index was less than 0.70 (64).

Challenge assay. Five 1-week-old SPF chickens in each group were inoculated with DMEM (0.2 ml each), IBDV/WT (10^4 PFU each), or IBDV/1FLAG (passage 30, 10^4 PFU each) through eye dropping. The chickens in each group were fed in one isolator. The titers of antibodies against IBDV in the serum were tested by ELISA at 0, 7, 14, and 21 days postinfection. Then, all the chickens were challenged with the virulent IBDV strain BC6/85 (2×10^4 EID_{50} each) by intranasal dropping at 21 days postinoculation. The chickens were observed daily for 10 days to evaluate the mortality, and the survival curves were generated according to the method of Kaplan-Meier.

Statistical analysis. All data were presented as mean ± standard deviation (SD) for each group and analyzed by SPSS 13.0 (IBM, Armonk, NY, USA). Two-tailed Student's *t* test was used to compare the mean between two groups. A *P* value of less than 0.05 was considered statistically significant.

ACKNOWLEDGMENTS

This study was supported by grants from the National Natural Science Foundation of China (31872501 and 31502061) and the Natural Science Foundation of Zhejiang Province (LY18C180002).

We appreciate the members in the lab of animal virology and immunology for their technical support. We also appreciate the valuable comments from anonymous reviewers and extend our thanks to Jinyang Zhang (Kunming University of Science and Technology) for critical reading of the manuscript.

H.Y. performed the animal experiments. Y.W. rescued and characterized the virus. C.Y. constructed the plasmids and evaluated the RNP activity. H.Y., Y.W., and C.Y. analyzed the data. C.Y. conceived the study, designed the experiments, drafted the figures, and wrote the paper.

REFERENCES

1. Rodríguez-Lecompte JC, Niño-Fong R, Lopez A, Markham RF, Kibenge FS. 2005. Infectious bursal disease virus (IBDV) induces apoptosis in chicken B cells. Comp Immunol Microbiol Infect Dis 28:321–337. https://doi.org/10.1016/j.cimid.2005.08.004.
2. Zhou X, Wang D, Xiong J, Zhang P, Li Y, She R. 2010. Protection of chickens, with or without maternal antibodies, against IBDV infection by a recombinant IBDV-VP2 protein. Vaccine 28:3990–3996. https://doi.org/10.1016/j.vaccine.2010.03.021.
3. Dobos P, Hill B, Hallett R, Kells D, Becht H, Teninges D. 1979. Biophysical and biochemical characterization of five animal viruses with bisegmented double-stranded RNA genomes. J Virol 32:593–605. https://doi.org/10.1128/JVI.32.2.593-605.1979.
4. von Einem UI, Gorbalenya AE, Schirrmeier H, Behrens S-E, Letzel T, Mundt E. 2004. VP1 of infectious bursal disease virus is an RNA-dependent RNA polymerase. J Gen Virol 85:2221–2229. https://doi.org/10.1099/vir.0.19772-0.
5. Calvert JG, Nagy E, Soler M, Dobos P. 1991. Characterization of the VPg-dsRNA linkage of infectious pancreatic necrosis virus. J Gen Virol 72:2563–2567. https://doi.org/10.1099/0022-1317-72-10-2563.
6. Kibenge FS, Dhama V. 1997. Evidence that virion-associated VP1 of avibirnaviruses contains viral RNA sequences. Arch Virol 142:1227–1236. https://doi.org/10.1007/s007050050154.
7. Müller H, Nitschke R. 1987. The two segments of the infectious bursal disease virus genome are circularized by a 90,000-Da protein. Virology 159:174–177. https://doi.org/10.1016/0042-6822(87)90363-1.
8. Escaffre O, Le Nouën C, Amelot M, Ambroggio X, Ogden KM, Guionie O, Toquin D, Müller H, Islam MR, Eterradossi N. 2013. Both genome segments contribute to the pathogenicity of very virulent infectious bursal disease virus. J Virol 87:2767–2780. https://doi.org/10.1128/JVI.02360-12.
9. Le Nouën C, Toquin D, Müller H, Raue R, Kean KM, Langlois P, Cherbonnel M, Eterradossi N. 2012. Different domains of the RNA polymerase of infectious bursal disease virus contribute to virulence. PLoS One 7:e28064. https://doi.org/10.1371/journal.pone.0028064.
10. Liu M, Vakharia VN. 2004. VP1 protein of infectious bursal disease virus modulates the virulence in vivo. Virology 330:62–73. https://doi.org/10.1016/j.virol.2004.09.009.
11. Yu F, Ren X, Wang Y, Qi X, Song J, Gao Y, Qin L, Gao H, Wang X. 2013. A single amino acid V4I substitution in VP1 attenuates virulence of very virulent infectious bursal disease virus (vvIBDV) in SPF chickens and increases replication in CEF cells. Virology 440:204–209. https://doi.org/10.1016/j.virol.2013.02.026.
12. Li Z, Wang Y, Xue Y, Li X, Cao H, Zheng SJ. 2012. Critical role for voltage-dependent anion channel 2 in infectious bursal disease virus-induced apoptosis in host cells via interaction with VP5. J Virol 86:1328–1338. https://doi.org/10.1128/JVI.06104-11.
13. Lombardo E, Maraver A, Espinosa I, Fernández-Arias A, Rodriguez JF. 2000. VP5, the nonstructural polypeptide of infectious bursal disease virus, accumulates within the host plasma membrane and induces cell lysis. Virology 277:345–357. https://doi.org/10.1006/viro.2000.0595.
14. Méndez F, de Garay T, Rodríguez D, Rodríguez JF. 2015. Infectious bursal disease virus VP5 polypeptide: a phosphoinositide-binding protein required for efficient cell-to-cell virus dissemination. PLoS One 10:e0123470. https://doi.org/10.1371/journal.pone.0123470.
15. Mundt E, Beyer J, Müller H. 1995. Identification of a novel viral protein in

infectious bursal disease virus-infected cells. J Gen Virol 76:437–443. https://doi.org/10.1099/0022-1317-76-2-437.
16. Mundt E, Köllner B, Kretzschmar D. 1997. VP5 of infectious bursal disease virus is not essential for viral replication in cell culture. J Virol 71:5647–5651. https://doi.org/10.1128/JVI.71.7.5647-5651.1997.
17. Wu Y, Hong L, Ye J, Huang Z, Zhou J. 2009. The VP5 protein of infectious bursal disease virus promotes virion release from infected cells and is not involved in cell death. Arch Virol 154:1873–1882. https://doi.org/10.1007/s00705-009-0524-4.
18. Da Costa B, Chevalier C, Henry C, Huet J-C, Petit S, Lepault J, Boot H, Delmas B. 2002. The capsid of infectious bursal disease virus contains several small peptides arising from the maturation process of pVP2. J Virol 76:2393–2402. https://doi.org/10.1128/jvi.76.5.2393-2402.2002.
19. Lejal N, Da Costa B, Huet JC, Delmas B. 2000. Role of Ser-652 and Lys-692 in the protease activity of infectious bursal disease virus VP4 and identification of its substrate cleavage sites. J Gen Virol 81:983–992. https://doi.org/10.1099/0022-1317-81-4-983.
20. Sánchez AB, Rodriguez JF. 1999. Proteolytic processing in infectious bursal disease virus: identification of the polyprotein cleavage sites by site-directed mutagenesis. Virology 262:190–199. https://doi.org/10.1006/viro.1999.9910.
21. Azad AA, Jagadish MN, Brown MA, Hudson PJ. 1987. Deletion mapping and expression in Escherichia coli of the large genomic segment of a birnavirus. Virology 161:145–152. https://doi.org/10.1016/0042-6822(87)90180-2.
22. Lee C-C, Ko T-P, Chou C-C, Yoshimura M, Doong S-R, Wang M-Y, Wang AH-J. 2006. Crystal structure of infectious bursal disease virus VP2 subviral particle at 2.6 Å resolution: implications in virion assembly and immunogenicity. J Struct Biol 155:74–86. https://doi.org/10.1016/j.jsb.2006.02.014.
23. Saugar I, Luque D, Oña A, Rodríguez JF, Carrascosa JL, Trus BL, Castón JR. 2005. Structural polymorphism of the major capsid protein of a double-stranded RNA virus: an amphipathic α helix as a molecular switch. Structure 13:1007–1017. https://doi.org/10.1016/j.str.2005.04.012.
24. Lombardo E, Maraver A, Castón JR, Rivera J, Fernández-Arias A, Serrano A, Carrascosa JL, Rodriguez JF. 1999. VP1, the putative RNA-dependent RNA polymerase of infectious bursal disease virus, forms complexes with the capsid protein VP3, leading to efficient encapsidation into virus-like particles. J Virol 73:6973–6983. https://doi.org/10.1128/JVI.73.8.6973-6983.1999.
25. Tacken MG, Peeters BP, Thomas AA, Rottier PJ, Boot HJ. 2002. Infectious bursal disease virus capsid protein VP3 interacts both with VP1, the RNA-dependent RNA polymerase, and with viral double-stranded RNA. J Virol 76:11301–11311. https://doi.org/10.1128/jvi.76.22.11301-11311.2002.
26. Dalton RM, Rodríguez JF. 2014. Rescue of infectious birnavirus from recombinant ribonucleoprotein complexes. PLoS One 9:e87790. https://doi.org/10.1371/journal.pone.0087790.
27. Ferrero D, Garriga D, Navarro A, Rodríguez JF, Verdaguer N. 2015. Infectious bursal disease virus VP3 upregulates VP1-mediated RNA-dependent RNA replication. J Virol 89:11165–11168. https://doi.org/10.1128/JVI.00218-15.
28. Ye C, Wang Y, Zhang E, Han X, Yu Z, Liu H. 2017. VP1 and VP3 are required and sufficient for translation initiation of uncapped infectious bursal disease virus genomic double-stranded RNA. J Virol 92:e01345-17. https://doi.org/10.1128/JVI.01345-17.
29. Li Z, Wang Y, Li X, Li X, Cao H, Zheng SJ. 2013. Critical roles of glucocorticoid-induced leucine zipper in infectious bursal disease virus (IBDV)-induced suppression of type I Interferon expression and enhancement of IBDV growth in host cells via interaction with VP4. J Virol 87:1221–1231. https://doi.org/10.1128/JVI.02421-12.
30. Ye C, Jia L, Sun Y, Hu B, Wang L, Lu X, Zhou J. 2014. Inhibition of antiviral innate immunity by birnavirus VP3 protein via blockage of viral double-stranded RNA binding to the host cytoplasmic RNA detector MDA5. J Virol 88:11154–11165. https://doi.org/10.1128/JVI.01115-14.
31. Ye C, Yu Z, Xiong Y, Wang Y, Ruan Y, Guo Y, Chen M, Luan S, Zhang E, Liu H. 2019. STAU1 binds to IBDV genomic double-stranded RNA and promotes viral replication via attenuation of MDA5-dependent beta interferon induction. FASEB J 33:286–300. https://doi.org/10.1096/fj.201800062RR.
32. Busnadiego I, Maestre AM, Rodriguez D, Rodriguez JF. 2012. The infectious bursal disease virus RNA-binding VP3 polypeptide inhibits PKR-mediated apoptosis. PLoS One 7:e46768. https://doi.org/10.1371/journal.pone.0046768.
33. Cubas-Gaona LL, Diaz-Beneitez E, Ciscar M, Rodríguez JF, Rodríguez D, Cubas-Gaona LL, Diaz-Beneitez E, Ciscar M, Rodríguez JF, Rodríguez D. 2018. Exacerbated apoptosis of cells infected with infectious bursal disease virus upon exposure to interferon alpha. J Virol 92:e00364-18. https://doi.org/10.1128/JVI.00364-18.
34. Jackwood DJ, Saif YM, Hughes JH. 1982. Characteristics and serologic studies of two serotypes of infectious bursal disease virus in turkeys. Avian Dis 26:871–882. https://doi.org/10.2307/1589875.
35. Cosgrove AS. 1962. An apparently new disease of chickens—avian nephrosis. Avian Dis 6:385–389. https://doi.org/10.2307/1587909.
36. Jackwood DH, Saif YM. 1987. Antigenic diversity of infectious bursal disease viruses. Avian Dis 31:766–770. https://doi.org/10.2307/1591028.
37. Chettle N, Stuart JC, Wyeth PJ. 1989. Outbreak of virulent infectious bursal disease in East Anglia. Vet Rec 125:271–272. https://doi.org/10.1136/vr.125.10.271.
38. Jackwood DJ, Sommer-Wagner S. 2007. Genetic characteristics of infectious bursal disease viruses from four continents. Virology 365:369–375. https://doi.org/10.1016/j.virol.2007.03.046.
39. Lim B-L, Cao Y, Yu T, Mo C-W. 1999. Adaptation of very virulent infectious bursal disease virus to chicken embryonic fibroblasts by site-directed mutagenesis of residues 279 and 284 of viral coat protein VP2. J Virol 73:2854–2862. https://doi.org/10.1128/JVI.73.4.2854-2862.1999.
40. Mundt E, de Haas N, van Loon AA. 2003. Development of a vaccine for immunization against classical as well as variant strains of infectious bursal disease virus using reverse genetics. Vaccine 21:4616–4624. https://doi.org/10.1016/s0264-410x(03)00448-1.
41. Quinlivan M, Zamarin D, García-Sastre A, Cullinane A, Chambers T, Palese P. 2005. Attenuation of equine influenza viruses through truncations of the NS1 protein. J Virol 79:8431–8439. https://doi.org/10.1128/JVI.79.13.8431-8439.2005.
42. Fan L, Wu T, Hussain A, Gao Y, Zeng X, Wang Y, Gao L, Li K, Wang Y, Liu C, Cui H, Pan Q, Zhang Y, Liu Y, He H, Wang X, Qi X. 2019. Novel variant strains of infectious bursal disease virus isolated in China. Vet Microbiol 230:212–220. https://doi.org/10.1016/j.vetmic.2019.01.023.
43. Perozo F, Villegas P, Fernandez R, Cruz J, Pritchard N. 2009. Efficacy of single dose recombinant herpesvirus of turkey infectious bursal disease virus (IBDV) vaccination against a variant IBDV strain. Avian Dis 53:624–628. https://doi.org/10.1637/8687-31009RESNOTE.1.
44. Huang Z, Elankumaran S, Yunus AS, Samal SK. 2004. A recombinant Newcastle disease virus (NDV) expressing VP2 protein of infectious bursal disease virus (IBDV) protects against NDV and IBDV. J Virol 78:10054–10063. https://doi.org/10.1128/JVI.78.18.10054-10063.2004.
45. Tsukamoto K, Kojima C, Komori Y, Tanimura N, Mase M, Yamaguchi S. 1999. Protection of chickens against very virulent infectious bursal disease virus (IBDV) and Marek's disease virus (MDV) with a recombinant MDV expressing IBDV VP2. Virology 257:352–362. https://doi.org/10.1006/viro.1999.9641.
46. Abdeljelil NB, Khabouchi N, Mardassi H. 2008. Efficient rescue of infectious bursal disease virus using a simplified RNA polymerase II-based reverse genetics strategy. Arch Virol 153:1131–1137. https://doi.org/10.1007/s00705-008-0080-3.
47. Boot HJ, Dokic K, Peeters BP. 2001. Comparison of RNA and cDNA transfection methods for rescue of infectious bursal disease virus. J Virol Methods 97:67–76. https://doi.org/10.1016/s0166-0934(01)00340-8.
48. Mundt E, Vakharia VN. 1996. Synthetic transcripts of double-stranded Birnavirus genome are infectious. Proc Natl Acad Sci U S A 93:11131–11136. https://doi.org/10.1073/pnas.93.20.11131.
49. Qi X, Gao Y, Gao H, Deng X, Bu Z, Wang X, Fu C, Wang X. 2007. An improved method for infectious bursal disease virus rescue using RNA polymerase II system. J Virol Methods 142:81–88. https://doi.org/10.1016/j.jviromet.2007.01.021.
50. Ortiz-Riano E, Cheng BYH, de la Torre JC, Martínez-Sobrido L. 2013. Arenavirus reverse genetics for vaccine development. J Gen Virol 94:1175–1188. https://doi.org/10.1099/vir.0.051102-0.
51. Makrides SC. 1999. Components of vectors for gene transfer and expression in mammalian cells. Protein Expr Purif 17:183–202. https://doi.org/10.1006/prep.1999.1137.
52. Wang Z, Day N, Trifillis P, Kiledjian M. 1999. An mRNA stability complex functions with poly (A)-binding protein to stabilize mRNA in vitro. Mol Cell Biol 19:4552–4560. https://doi.org/10.1128/MCB.19.7.4552.
53. Li K, Liu Y, Zhang Y, Gao L, Liu C, Cui H, Qi X, Gao Y, Zhong L, Wang X. 2017. Protective efficacy of a novel recombinant Marek's disease virus vector vaccine against infectious bursal disease in chickens with or without maternal antibodies. Vet Immunol Immunopathol 186:55–59. https://doi.org/10.1016/j.vetimm.2017.02.003.

54. Hoffmann E, Neumann G, Kawaoka Y, Hobom G, Webster RG. 2000. A DNA transfection system for generation of influenza A virus from eight plasmids. Proc Natl Acad Sci U S A 97:6108–6113. https://doi.org/10.1073/pnas.100133697.
55. Hoffmann E, Webster RG. 2000. Unidirectional RNA polymerase I-polymerase II transcription system for the generation of influenza A virus from eight plasmids. J Gen Virol 81:2843–2847. https://doi.org/10.1099/0022-1317-81-12-2843.
56. Grummt I, Roth E, Paule MR. 1982. Ribosomal RNA transcription in vitro is species specific. Nature 296:173–174. https://doi.org/10.1038/296173a0.
57. Martínez-Sobrido L, Emonet S, Giannakas P, Cubitt B, García-Sastre A, de la Torre JC. 2009. Identification of amino acid residues critical for the anti-interferon activity of the nucleoprotein of the prototypic arenavirus lymphocytic choriomeningitis virus. J Virol 83:11330–11340. https://doi.org/10.1128/JVI.00763-09.
58. Sánchez AB, de la Torre JC. 2005. Genetic and biochemical evidence for an oligomeric structure of the functional L polymerase of the prototypic arenavirus lymphocytic choriomeningitis virus. J Virol 79:7262–7268. https://doi.org/10.1128/JVI.79.11.7262-7268.2005.
59. Ye C, Han X, Yu Z, Zhang E, Wang L, Liu H. 2017. Infectious bursal disease virus activates c-Src to promote $\alpha 4\beta 1$ integrin-dependent viral entry by modulating the downstream Akt-RhoA GTPase-actin rearrangement cascade. J Virol 91:e01891-16. https://doi.org/10.1128/JVI.01891-16.
60. Gao L, Qi X, Li K, Gao H, Gao Y, Qin L, Wang Y, Wang X. 2011. Development of a tailored vaccine against challenge with very virulent infectious bursal disease virus of chickens using reverse genetics. Vaccine 29:5550–5557. https://doi.org/10.1016/j.vaccine.2011.04.106.
61. Mosley YYC, Wu CC, Lin TL. 2014. An influenza A virus hemagglutinin (HA) epitope inserted in and expressed from several loci of the infectious bursal disease virus genome induces HA-specific antibodies. Arch Virol 159:2033–2041. https://doi.org/10.1007/s00705-014-2036-0.
62. Hemsley A, Arnheim N, Toney MD, Cortopassi G, Galas DJ. 1989. A simple method for site-directed mutagenesis using the polymerase chain reaction. Nucleic Acids Res 17:6545–6551. https://doi.org/10.1093/nar/17.16.6545.
63. Luque D, Rivas G, Alfonso C, Carrascosa JL, Rodríguez JF, Castón JR. 2009. Infectious bursal disease virus is an icosahedral polyploid dsRNA virus. Proc Natl Acad Sci U S A 106:2148–2152. https://doi.org/10.1073/pnas.0808498106.
64. Lucio B, Hitchner SB. 1979. Infectious bursal disease emulsified vaccine: effect upon neutralizing-antibody levels in the dam and subsequent protection of the progeny. Avian Dis 23:466–478. https://doi.org/10.2307/1589577.